

# UC Irvine

## UC Irvine Previously Published Works

### Title

AAV8-Mediated Gene Therapy Rescues Retinal Degeneration Phenotype in a Tlcd3b Knockout Mouse Model.

### Permalink

<https://escholarship.org/uc/item/3fp1j0n4>

### Journal

Investigative Ophthalmology & Visual Science, 63(3)

### Authors

Qian, Xinye

Liu, Hehe

Fu, Shangyi

et al.

### Publication Date

2022-03-02

### DOI

10.1167/iovs.63.3.11

Peer reviewed

# AAV8-Mediated Gene Therapy Rescues Retinal Degeneration Phenotype in a *Tlcd3b* Knockout Mouse Model

Xinye Qian,<sup>1,2</sup> Hehe Liu,<sup>2</sup> Shangyi Fu,<sup>2,3</sup> Jiaxiong Lu,<sup>1,2</sup> Yu-Ting Hung,<sup>4</sup> Cassidy Turner,<sup>4</sup> Haiwei Gu,<sup>4</sup> and Rui Chen<sup>2,5</sup>

<sup>1</sup>Verna and Marrs McLean Department of Biochemistry and Molecular Biology, Baylor College of Medicine, Houston, Texas, United States

<sup>2</sup>Human Genome Sequencing Center, Baylor College of Medicine, Houston, Texas, United States

<sup>3</sup>School of Medicine, Baylor College of Medicine, Houston, Texas, United States

<sup>4</sup>Arizona Metabolomics Laboratory, College of Health Solutions, Arizona State University, Scottsdale, Arizona, United States

<sup>5</sup>Department of Molecular and Human Genetics, Baylor College of Medicine, Houston, Texas, United States

Correspondence: Rui Chen, Baylor College of Medicine, T836, 1 Baylor Plaza, Houston, TX 77030, USA; [ruichen@bcm.edu](mailto:ruichen@bcm.edu).

**Received:** October 20, 2021

**Accepted:** February 22, 2022

**Published:** March 11, 2022

Citation: Qian X, Liu H, Fu S, et al. AAV8-mediated gene therapy rescues retinal degeneration phenotype in a *Tlcd3b* knockout mouse model. *Invest Ophthalmol Vis Sci.* 2022;63(3):11. <https://doi.org/10.1167/iovs.63.3.11>

**PURPOSE.** The purpose of this study was to assess the therapeutic efficacy of *rAAV8-bGRK1-Tlcd3b* in a *Tlcd3b*<sup>-/-</sup> mouse model of retinal degeneration and validate TLCD3B's role as a ceramide synthase in vivo.

**METHODS.** Using *Tlcd3b*<sup>-/-</sup> mice as an inherited retinal disease animal model, we performed subretinal injection of *rAAV8-bGRK1-Tlcd3b* and evaluated the efficacy of gene replacement therapy. *Tlcd3b*<sup>-/-</sup> mice were treated at two time points: postnatal day 21 (P21) and postnatal day 120 (P120) with various dosages.

**RESULTS.** *Tlcd3b* overexpression rescued retinal degeneration in the mutant mice, as indicated by significantly improved photoreceptor function and preservation of photoreceptor cells over the course of 1 year. Although *Tlcd3b* is expressed in all cell types in the retina, photoreceptor cell-specific expression of *Tlcd3b* is sufficient to rescue the phenotype, indicating the primary function of TLCD3B is in photoreceptors. Consistent with the idea that TLCD3B is a ceramide synthase, mass spectrometry analyses of the mutant retina indicate the reduction of C16-, C18-, and C20-ceramides in the retina, which are restored with *Tlcd3b* overexpression.

**CONCLUSIONS.** Our findings demonstrated the therapeutic efficacy of gene therapy in treating *Tlcd3b* mutant retina, laying the foundation for developing future therapy for *TLCD3B* retinopathy.

**Keywords:** inherited retinal dystrophy, TLCD3B, ceramide, ceramide synthase, gene therapy

Ceramide is the component lipid that makes up sphingomyelin, which is one of the major lipids in the lipid bilayer. Evidence from both in vitro and in vivo studies has supported ceramide's role as an essential second messenger in the activation of apoptosis in photoreceptors, which is the hallmark of most retinal degenerative disorders.<sup>1-3</sup> Interestingly, both high and low levels of ceramides have been linked to apoptosis. The work of several groups has shown that the accumulation of ceramides, arising from the activation of different biosynthetic pathways, emerges as a death arbitrator in photoreceptors.<sup>4-8</sup> Reduced ceramide levels, however, have been previously linked to neurodegeneration in the cerebellum of *CerS1*-deficient mice.<sup>9</sup> Although it is known that the maintenance of ceramide homeostasis is important for retinal cell survival,<sup>4-9</sup> the roles of ceramides are not well studied in the retina.

Ceramide is generated through four pathways, de novo synthesis, the salvage pathway, the sphingomyelinase pathway, and the ceramide-recycling pathway, where

ceramide synthases participate in all but the sphingomyelinase pathway.<sup>10,11</sup> There are six ceramide synthase (CerS) isoforms, CerS1-6, in mammals,<sup>11</sup> and different isoforms generate ceramides with distinct acyl chain lengths, thus generating different molecular species of ceramides with distinct cellular effects.<sup>7,12,13</sup> Besides the six canonical ceramide synthases, a newly identified ceramide synthase, TLCD3B, was shown to synthesize C16-, C18-, and C20-ceramides in vitro.<sup>14</sup> We identified a frameshift mutation (p. Gln79Asnfs\*43) and a missense mutation (p. Gly56Ser) in *TLCD3B*, which encodes TLC domain-containing protein 3B, in patients diagnosed with autosomal recessive CRD (Cone-rod Dystrophy) and maculopathy.<sup>15</sup> Both mutations were predicted to lead to *TLCD3B* loss of function. Patients with these *TLCD3B* mutations showed clinical signs of cone photoreceptor degeneration and predominant cone system dysfunction.<sup>15</sup>

A *Tlcd3b* knockout (*Tlcd3b*<sup>-/-</sup>) mouse was generated to model the pathogenesis of *TLCD3B* retinopathy. Consistent

with the patient phenotype, *Tlcd3b* deletion in mice leads to cone photoreceptor dysfunction and degeneration.<sup>15</sup> At 7 months old, a reduction in outer nuclear layer (ONL) thickness and cone photoreceptor cell number is observed in *Tlcd3b*<sup>-/-</sup> mouse retina compared to controls at 20% and 30%, respectively.<sup>15</sup> Concerning the wide time window of disease progression, the *Tlcd3b*<sup>-/-</sup> mouse model is an ideal candidate for gene therapy as most photoreceptors are present and functional in early staged mice.

During the past decade, exciting progress has been made in the field of gene therapy study to correct the genetic defects that lead to nonsyndromic retinal dystrophies. Specifically, recombinant adeno-associated virus (rAAV)-based gene therapies, enabling efficient delivery of functional genes into mutant eyes and the rescue of disease phenotypes, have been shown to be a successful treatment method in both animal models of retinal degeneration<sup>16-27</sup> and patients.<sup>28-32</sup> Indeed, RPE65 gene therapy has been approved by the US Food and Drug Administration as the first gene therapy for patients with Leber congenital amaurosis 2 (OMIM entry MIM204100) and retinitis pigmentosa 20 (MIM#613794).

In this study, using *Tlcd3b*<sup>-/-</sup> mice as the model, we performed subretinal injections of *rAAV8-hGRK1-Tlcd3b* and evaluated the efficacy of gene replacement therapy. Among the various serotypes, a tyrosine-capsid mutant adeno-associated virus (AAV) vector plasmid, AAV8(Y733F), has been studied extensively to achieve high transduction efficiency, more rapid transgene expression, cell transduction specificity, and stable and long-term expression in photoreceptor cells.<sup>26,27,33-35</sup> As expected, the gene therapy significantly improved photoreceptor function and preservation of photoreceptor cells over a course of 1 year upon expression of *rAAV8-Tlcd3b* in the mutant retina. Consistent with the idea that TLCD3B is a ceramide synthase, mass spectrometry analyses of the mutant retina indicate the reduction of C16-, C18-, and C20-ceramides in the retina, which is restored by *rAAV8-Tlcd3b* expression. Taken together, our results demonstrate the feasibility of gene replacement therapy in treating the *Tlcd3b* knockout retinal disease mouse model. Therefore, given the conservation between humans and mice, this work lays a foundation for the potential gene therapy treatment in humans with retinal pathologies associated with *TLCD3B* mutations.

## MATERIALS AND METHODS

### Production of *rAAV8-Tlcd3b* Viral Vector

Full-length *Tlcd3b* cDNA (Origene #MC210825; NM\_029978.1) was sequence-verified and amplified by PCR. For exogenous *Tlcd3b* transgene expression detection, a FLAG tag was added at the N-terminus of the *Tlcd3b* gene during the PCR amplification using a primer set that includes the sequences of the FLAG tag and restriction enzyme sites AgeI and EcoRI at the end (forward primer: GGACCG-GTGCCACCATGCTTACCCCAATGGTGGC; reverse primer: GGGAAATTCTCACTTATCGTCGTCATCCTTGTAATCTCAGTC-CTGGGTCTGACAA). Both the pTR-hGRK1 AAV vector (see vector map in Supplementary Fig. S1) and the PCR-amplified cDNA were digested with AgeI and EcoRI. The digested vector was gel-purified and then ligated with the digested insert. For AAV packaging, *rAAV8* was used for packaging *Grk1-Tlcd3b* to achieve robust transduction efficiency and expression in retinal photoreceptors (Gene Vector Core, Baylor College of Medicine).

## Animals

*Tlcd3b*<sup>-/-</sup> mice were generated as previously described<sup>15</sup> and maintained on a C57BL/6J genetic background. All mice in this study were maintained in a 14-hour light/10-hour dark cyclic environment. All animal operations were approved by the Institutional Animal Care and Use Committee at Baylor College of Medicine.

## Subretinal Injection

Postnatal day 21 (P21) and postnatal day 120 (P120) mice were anesthetized with a combination drug consisting of ketamine (22 mg/kg), xylazine (4.4 mg/kg), and acepromazine (0.37 mg/kg), which was injected intraperitoneally. Subretinal injections were performed as described previously.<sup>36</sup> A shallow incision was made through the sclera with a beveled 30-gauge needle. A 32-gauge blunt needle was presented inside the vitreous cavity and pushed forward until the tip of the needle had moved past the retina. The viral solution was injected into the subretinal space using an Ultra-Micro-Pump II and Micron-4 Controller (World Precision Instruments, Sarasota, Florida). All mice were treated once into the subretinal space with 1  $\mu$ L *rAAV8-hGRK1-Tlcd3b* in the right eye, whereas the contralateral left eye was injected subretinally with 1  $\mu$ L PBS, serving as an internal control, while age-matched wild types were used as the external controls. All animal phenotyping materials and methods are standard procedure and can be found in the Supplementary Materials and Methods.

## RESULTS

### AAV-Mediated *Tlcd3b* Expression in Photoreceptor Cells

The primary defect observed in patients and mice in the absence of TLCD3B function is photoreceptor degeneration. Therefore, we reason that it is likely that the targeted expression of *Tlcd3b* cDNA in photoreceptor cells is sufficient to rescue the mutant phenotype. To target *Tlcd3b* expression in photoreceptor cells, we cloned mouse *Tlcd3b* cDNA under the control of the human rhodopsin kinase (hGRK1) promoter and then packaged the construct in *rAAV8*. Since *Tlcd3b*<sup>-/-</sup> mice have a late onset of photoreceptor degeneration starting at 7 months, we performed subretinal injections of *rAAV8-Tlcd3b* at P21. To test if the effect of the timing of treatment, we also treated *Tlcd3b*<sup>-/-</sup> mice at a late time point of P120. In this study, all treatments were performed in the right eye (RE), and the contralateral left eye (LE) was injected with PBS, serving as the internal control.

Two months after the injection, we collected both eyes of injected mutant mice and examined their retina by immunofluorescence staining. In *Tlcd3b*<sup>-/-</sup> mice, as expected, TLCD3B protein was not detected in the untreated LE (Fig. 1A). In contrast, the expression of TLCD3B, which extended throughout most of the retina, was observed in the treated RE (Fig. 1A). At a higher magnification, TLCD3B immunolabeling was detected specifically in the photoreceptors of the treated retina, where it colocalized with FLAG-positive staining (Fig. 1B). Taken together, the *rAAV8-Tlcd3b* vector resulted in a stable and specific expression of TLCD3B in photoreceptors upon treatment.

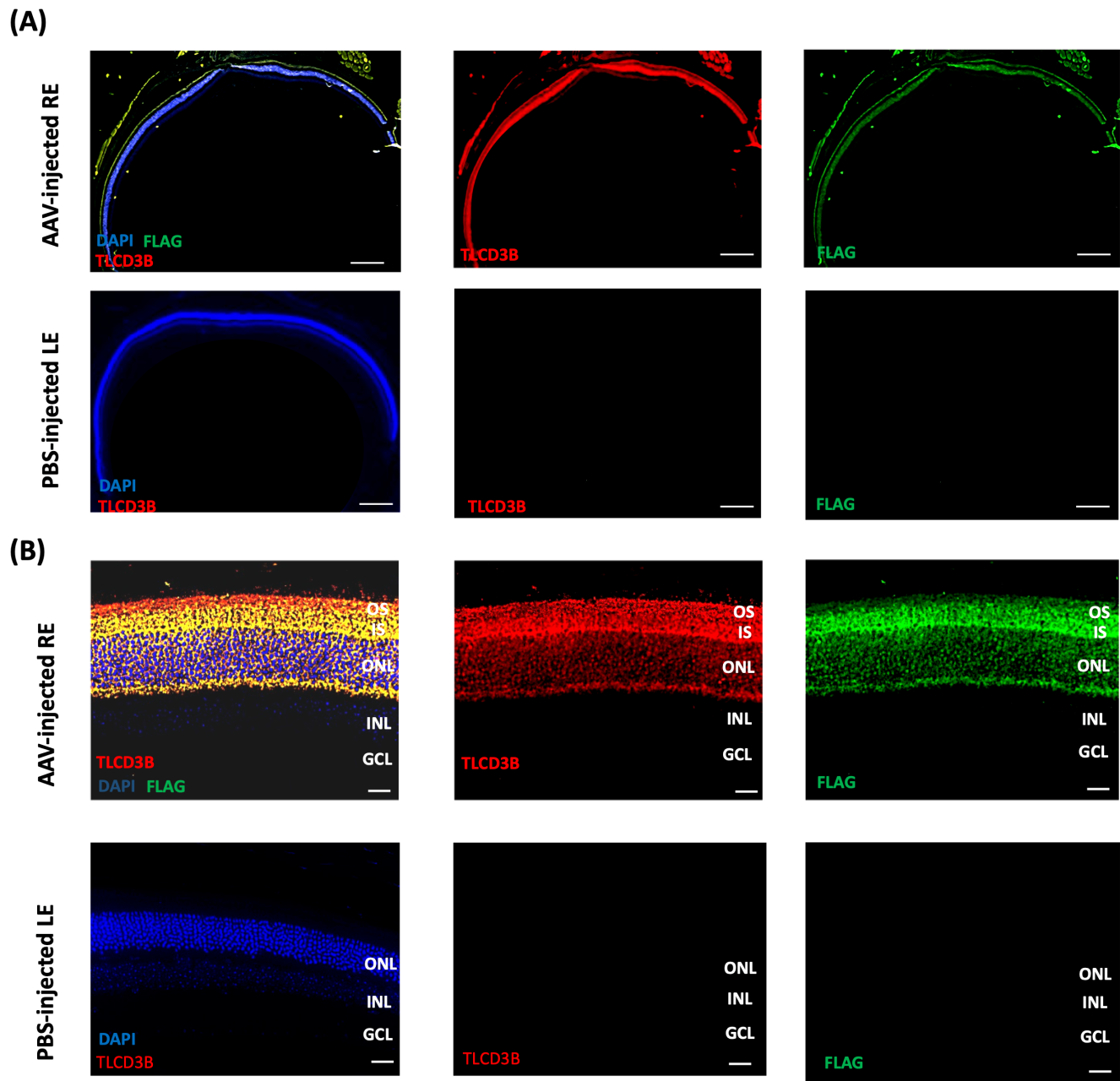


**FIGURE 1.** *AAV8-Tlcd3b* transgene expression was verified in the *rAAV8-Tlcd3b*-treated retina of *Tlcd3b*<sup>-/-</sup> mice. **(A, B)** Immunofluorescence staining of representative contralateral untreated LE of *Tlcd3b*<sup>-/-</sup> mouse retina and treated RE of *Tlcd3b*<sup>-/-</sup> mouse retina at 2 months postinjection performed on postnatal day 21. TLCD3B and FLAG staining was undetectable in the PBS-injected LE of *Tlcd3b*<sup>-/-</sup> mice, whereas in the treated RE, robust staining was detected in the outer segment, the inner segment, and the outer nuclear layer of the retina. DAPI staining was performed to stain for cell nuclei. **Scale bar:** **(A)** 500  $\mu$ m, **(B)** 20  $\mu$ m. GCL, ganglion cell layer; INL, inner nuclear layer; IPL, inner plexiform layer; IS, inner segment; OPL, outer plexiform layer; OS, outer segment.

### Improvement in Photoreceptor Function in *rAAV8-Tlcd3b*-Treated *Tlcd3b* Mutant Mice

We next tested whether *rAAV8-Tlcd3b* treatment could rescue photoresponses in *Tlcd3b*<sup>-/-</sup> mice. To determine if there is any functional rescue of electrophysiologic responses to light in *Tlcd3b*<sup>-/-</sup> mice, we examined the ERGs of dark-adapted *Tlcd3b*<sup>-/-</sup> mice by testing LE and RE responses independently.

At 7 months of age, *Tlcd3b*<sup>-/-</sup> mice exhibited significantly reduced scotopic and photopic b-wave amplitude in

the contralateral untreated LE compared with the wild-type control mice (Fig. 2), indicating cone photoreceptor and bipolar dysfunction, while scotopic a-wave ERGs showed a normal response of rod photoreceptors. In both P21- and P120-treated *Tlcd3b*<sup>-/-</sup> mice, at a concentration of  $1.03 \times 10^{12}$  g.c./mL (genome copies/mL) of *rAAV8-Tlcd3b*, the treated RE (Fig. 2) had significant improvements in both the scotopic and photopic b-wave responses, indicating functional improvement in cone photoreceptor cells and photo-transduction/inner retinal neurons' response. Nevertheless, an earlier treatment at P21 had a slightly better rescue

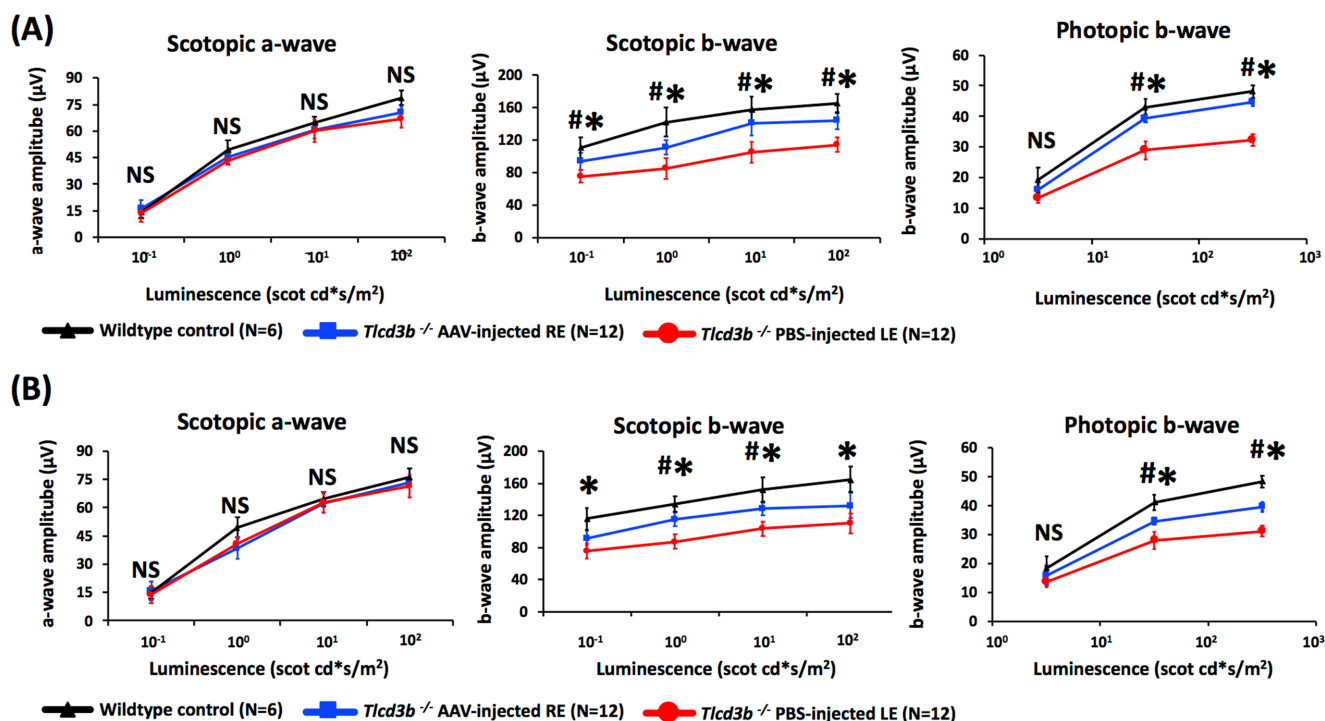


**FIGURE 2.** ERG analysis demonstrated functional improvement in 7-month-old *rAAV8-Tlcd3b*-treated *Tlcd3b*<sup>-/-</sup> mice injected at (A) P21 and (B) P120. Two-way ANOVA tests on electroretinography on (A) P21- and (B) P120-injected 7-month-old mice showed unaffected scotopic a-wave ( $P = 0.67$  for P21-injected mice;  $P = 0.42$  for P120-injected mice) and significantly elevated scotopic ( $P = 0.01$  for P21-injected mice;  $P = 0.03$  for P120-injected mice) and photopic b-waves ( $P = 0.003$  for P21-injected mice;  $P = 0.008$  for P120-injected mice) in AAV-treated RE (blue lines) compared with untreated, PBS-injected LE (red lines). In addition, results of untreated wild-type (WT) age-matched mice (black line) are included for comparison, and there was no significant difference between the a-wave and b-wave amplitudes of WT and AAV-injected mice for both P21- and P120-treated groups. Significance at each luminescence was determined by Student's *t*-test. Error bars denote the SEM. NS, not significant; wild-type versus PBS-injected ( $*P < 0.05$ ) and PBS-injected versus AAV-treated ( $\#P < 0.05$ ). AAV-treated RE (blue line), PBS-treated LE (red line), and WT control (black line).

efficacy than the later treatment at P120 (Supplementary Fig. S2A).

As significantly improved ERGs are observed at 7 months old for both P21- and P120-treated *Tlcd3b* mutant mice using a concentration of  $1.03 \times 10^{12}$  g.c./mL, we also tested if the rescue effect is dosage dependent. Treatment with a dosage of  $1.03 \times 10^{11}$  g.c./mL showed slightly increased scotopic and photopic b-wave amplitudes in treated REs compared to PBS-injected LEs, while the  $1.03 \times 10^{10}$  g.c./mL treatment showed no significant improvement in ERG b-waves (Supplementary Fig. S3). Similarly, a treatment dosage of  $1.03 \times 10^{12}$  g.c./mL also demonstrated the best rescue effect in terms of retinal morphology, as evident by most significantly increased ONL thickness (Supplementary Fig. S4). Based on these results, the dosage of  $1.03 \times 10^{12}$  g.c./mL was used for all subsequent experiments.

### Targeted Expression of *Tlcd3b* in Photoreceptor Cells Rescues the Degeneration Phenotype Due to *Tlcd3b* Mutation

Consistent with the improved performance of the photoreceptors and interneurons measured by ERGs, a significant morphologic preservation was observed in P21 or P120 *rAAV8-Tlcd3b*-treated *Tlcd3b*<sup>-/-</sup> mice. At 7 months old, *Tlcd3b*<sup>-/-</sup> mice (indicated by untreated LE) exhibited significant overall retinal thickness reduction and ONL thinning

compared to the wild-type control (Figs. 3A, 3B). H&E staining of retinal sections at 7 months old showed that treatments at P21 and P120 both led to significant improvements in retinal morphology ( $P = 0.006$  for P21-treated group and  $P = 0.01$  for P120-treated group), as evident by the preservation of photoreceptor cell nuclei in the ONL (Figs. 3A, 3B). There was about a 20% reduction in the ONL thickness of the untreated LE of *Tlcd3b*<sup>-/-</sup> mice compared to the wild-type control. In contrast, the ONL thickness of P21-treated RE retinas (Fig. 3C) was at approximately 95% of the wild type, while the ONL thickness of P120-treated RE retinas (Fig. 3D) also had only a 10% reduction compared to the wild-type retina, indicating successful preservation of photoreceptor in treated mutant mice.

As *Tlcd3b*<sup>-/-</sup> mice were reported to have a 30% loss of cones in mutant retinas compared with wild-type retinas at 7 months old,<sup>15</sup> we also looked at cone photoreceptors to examine if cone cells are well preserved in the treated mutant mice. Retinal cross sections of the treated REs of *Tlcd3b*<sup>-/-</sup> mice showed well-preserved cone outer and inner segments and axon terminal morphology, as well as an increased number of cones in both the inner and outer segments compared with that of the untreated LE retina (Figs. 4A–D). We also conducted peanut agglutinin (PNA) staining on retinal wholemounts to accurately determine the cone degeneration phenotype. Overall, there was a significantly increased number of PNA-positive cone cells 6 months after subretinal injection at P21 (Figs. 4E, 4F), as

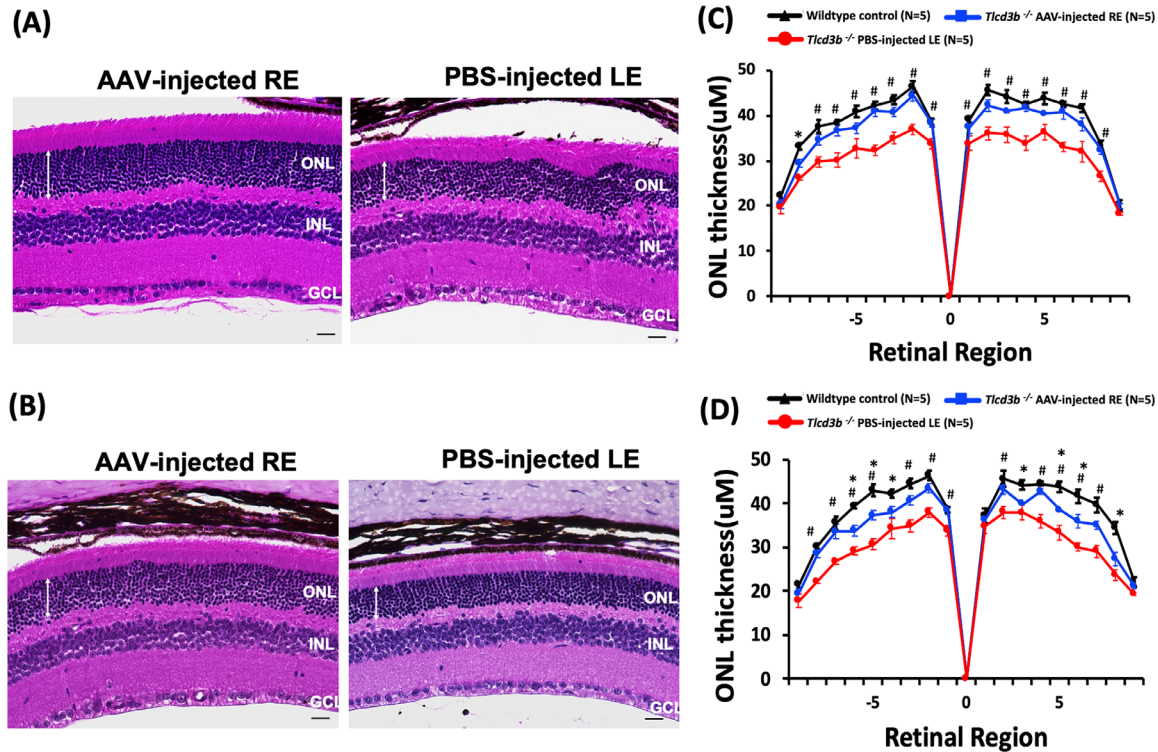


**FIGURE 3.** Preservation of photoreceptor morphology in treated *Tlcd3b*<sup>-/-</sup> mice at 7 months old. Hematoxylin and eosin staining of paraffin-embedded retinal sections was performed to assess morphologic changes in the untreated LE and treated RE of 7-month-old *Tlcd3b*<sup>-/-</sup> mice that were injected at (A) P21 and (B) P120. Scale bar: 50 µm. The butterfly plot includes ONL thickness measured from 18 equally spaced positions along the vertical median of the retina collected 6 months after P21 injection (C) and 3 months after P120 injection (D). Each dot represents an individual data point plotted over mean ± SEM. Position 0 corresponds to the optic nerve head. Error bars denote the SEM. Wild-type versus AAV-injected (\**P* < 0.05) and PBS-injected versus AAV-treated (#*P* < 0.05). For both P21- and P120-treated mice, no significant difference between the ONL thickness of AAV-treated RE and age-matched WT controls. AAV-treated RE (blue line), PBS-treated LE (red line), and WT control (black line).

the cone cell density was increased by approximately 33% in the treated RE retina compared to the untreated LE retina. Similarly, the number of PNA-positive cone cells significantly increased by approximately 22% in the 7-month-old P120-injected *Tlcd3b*<sup>-/-</sup> mice (Figs. 4E, 4F).

### Long-Term Rescue Efficiency of *rAAV8-Tlcd3b*-Mediated Gene Therapy in *Tlcd3b*<sup>-/-</sup> Mice

Both P21- and P120-treated *Tlcd3b*<sup>-/-</sup> mice were examined at the 1-year time point to assess the long-term rescue potential of *rAAV8-Tlcd3b* gene therapy treatment. Functional improvement was consistently observed at 1 year, as measured by ERGs in dark-adapted *Tlcd3b*<sup>-/-</sup> mice (Figs. 5A, 5B). In 1-year-old *Tlcd3b*<sup>-/-</sup> mice, LEs exhibited a significantly reduced a-wave amplitude compared to the wild type, indicating significant rod photoreceptor dysfunctions at the late stage. Both scotopic and photopic b-wave responses of LEs were further diminished compared to those at 7 months old. REs of both P21 and P120 *Tlcd3b*<sup>-/-</sup> mice demonstrated significantly increased a-wave and b-wave amplitudes compared to LEs, indicating successful preservation of photoreceptor and interneuron functions up to 1 year.

Besides retaining photoresponses, *Tlcd3b*<sup>-/-</sup> mouse REs also maintained a better retinal morphology, as measured

by histologic analyses (Figs. 5C–H). In 1-year-old *Tlcd3b*<sup>-/-</sup> mice, the LE retina ONL was further reduced to 60% of the wild-type retina ONL, suggesting a progressive photoreceptor degeneration after the degeneration onset at 7 months old (Figs. 5C–F). Both P21- and P120-treated RE retinas of *Tlcd3b*<sup>-/-</sup> mice, however, demonstrated a significantly thicker ONL compared to the untreated LEs, indicating significant retention of the photoreceptor integrity after prolonged treatment. Additionally, cone cells were better preserved in outer and inner segments as well as at synaptic terminals of the treated RE retina compared to the untreated LE retina of 1-year-old *Tlcd3b*<sup>-/-</sup> mice (Figs. 5G, 5H), indicating that the *rAAV8-Tlcd3b* treatment is capable of long-term preservation of cone photoreceptors for at least 11 months after treatment.

Despite the normal scotopic a-wave and impaired scotopic b-wave responses, *Tlcd3b*<sup>-/-</sup> mice had an insignificant thinning of the inner nuclear layer across the retina at 7 months of age, and no significant changes were observed for cell number or morphology of rod-bipolar cells.<sup>15</sup> Although at both 7 month-old (7M) and 12 month-old (12M), *Tlcd3b*<sup>-/-</sup> mice did not show significant changes in rod-bipolar cell morphology (Supplementary Fig. S5), it was evident that RIBEYE immunoreactive spots greatly decreased, indicating a loss of contact between photoreceptor and bipolar cells at 12M (Supplementary Fig. S5B). Meanwhile, both the P21 and P120 gene therapy treatments led to a better preservation of synapses, as evident by the more

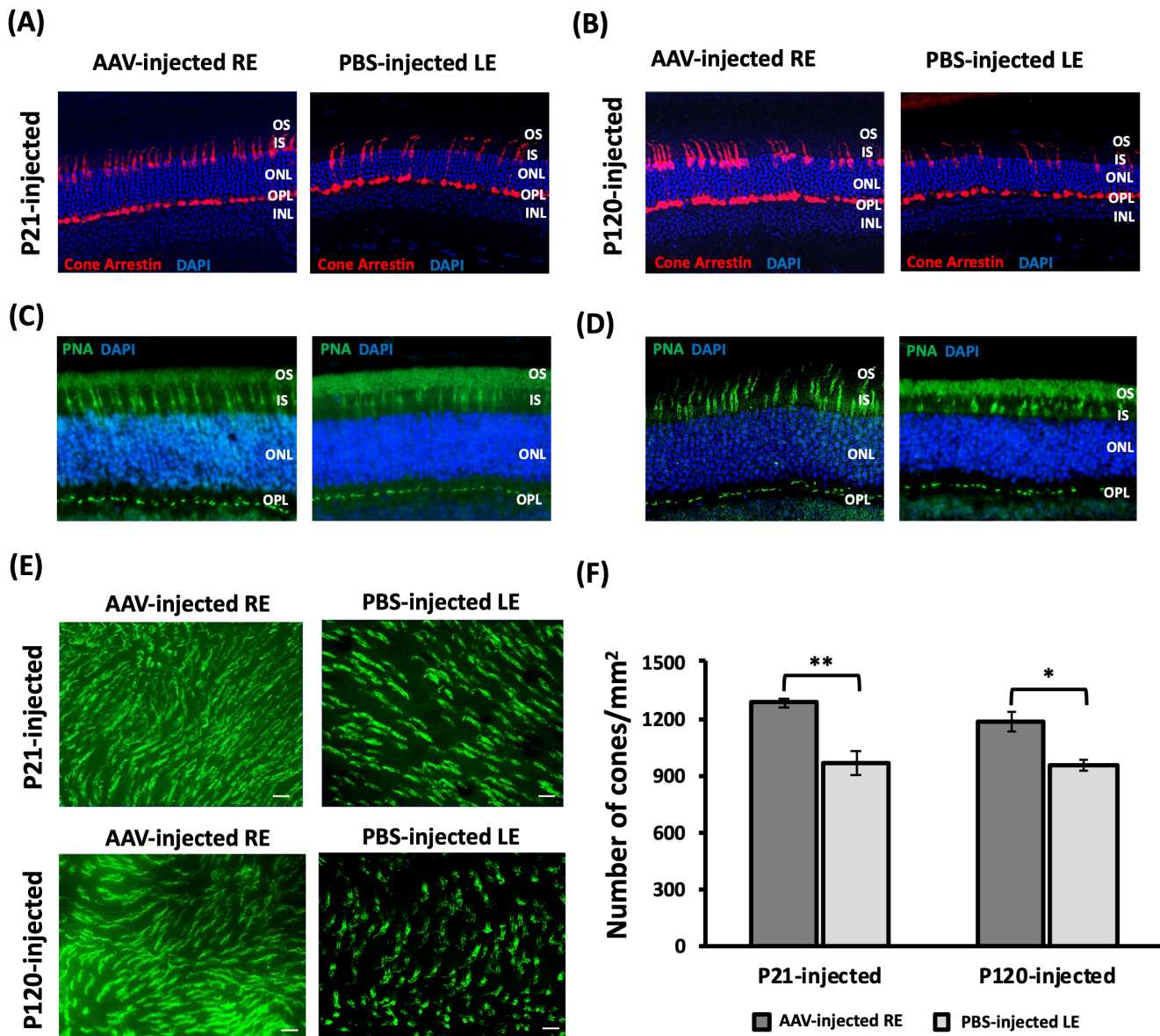


**FIGURE 4.** Assessment of cone morphology preservation in 7-month-old *rAAV8-Tlcd3b*-treated *Tlcd3b*<sup>-/-</sup> mice. Immunofluorescent staining of cone arrestin (red; **A, B**) and PNA (green; **C, D**) on cross sections of representative contralateral untreated LE and treated RE of *Tlcd3b*<sup>-/-</sup> mouse retina at 6 months postinjection performed on (**A, C**) P21 and (**B, D**) 3 months postinjection performed on P120. (**E**) In 7-month-old P21- and P120-injected *Tlcd3b*<sup>-/-</sup> mice, PNA staining (green) shows loss of cones compared with wild type in retinal whole mounts. Scale bar: 20  $\mu$ m. (**F**) Cones were counted in the dorsonasal (DN), dorsotemporal (DT), ventronasal (VN), and ventrotemporal (VT) regions of (**E**) PNA-stained (green) retinal whole mounts of treated RE ( $n = 4$ ) and untreated LE ( $n = 4$ ) and then expressed as average number of cones per mm<sup>2</sup> (mean  $\pm$  SEM). \* $P < 0.05$ , \*\* $P < 0.01$ , \*\*\* $P < 0.001$ . IS, inner segment; OS, outer segment.

robust RIBEYE staining in the AAV-treated RE compared to the contralateral control eye (Supplementary Fig. S5).

In terms of long-term rescue efficiency, although we observed successful preservation in both treatment groups, it is evident that an earlier treatment at P21 had a better rescue potential at 1 year old compared to the later treatment at P120, as indicated by more improved photoreponses (Supplementary Fig. S2B) and a better-preserved retinal morphology. The ONL thickness of P21-treated RE retinas was at approximately 90% of the wild type (Fig. 5D), which did not differ much from the results at 7 months old (Fig. 3C). The ONL thickness of P120-treated RE reti-

nas (Fig. 5F), however, only maintained approximately 78% of the wild-type retina.

#### *rAAV8-Tlcd3b*-Mediated Gene Therapy Recovers the Level of Different Ceramide Species in *Tlcd3b*<sup>-/-</sup> Mice

To investigate whether the *rAAV8-Tlcd3b* gene therapy alters the sphingolipid composition in the retina, we performed mass spectrometry analyses of different ceramide subtypes and sphingosine in retinas of LEs and REs of P21-injected

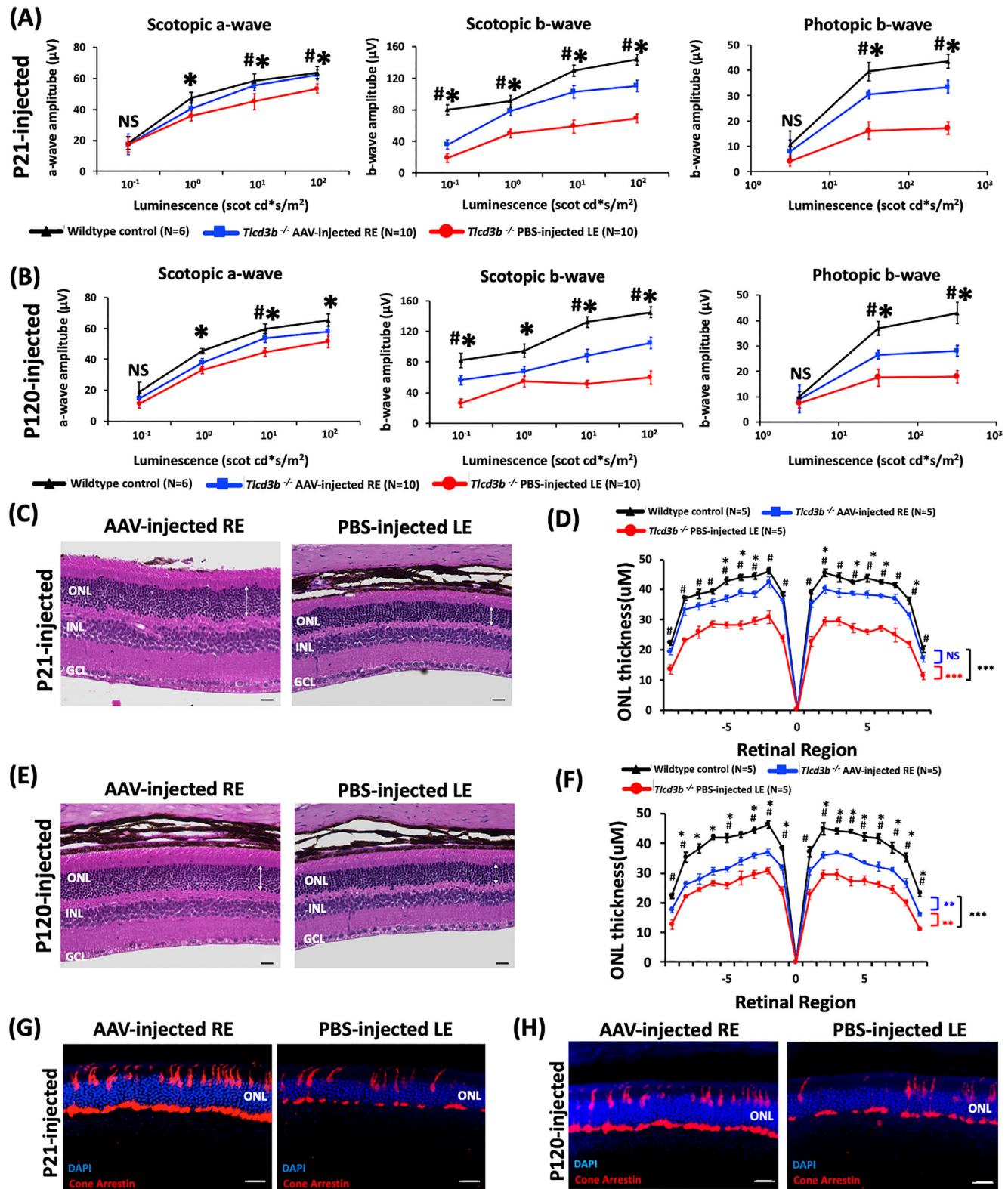


**FIGURE 5.** Long-term rescue efficiency of rAAV8-*Tlcd3b*-mediated gene therapy in *Tlcd3b*<sup>-/-</sup> mice. Two-way ANOVA analysis on ERG data demonstrated functional improvement in RE (blue line) compared with the LE (red line) of both (A) P21-injected and (B) P120-injected 1-year-old *Tlcd3b*<sup>-/-</sup> mice, as indicated by the significantly elevated scotopic ( $P = 0.004$  for P21-injected mice;  $P = 0.01$  for P120-injected mice) and photopic b-waves ( $P = 0.0001$  for P21-injected mice;  $P = 0.006$  for P120-injected mice) in the treated eyes compared with the untreated eyes. Significance at each luminescence was determined by Student's *t*-test. Error bars denote the SEM. Wild-type versus PBS-injected ( $*P < 0.05$ ) and PBS-injected versus AAV-treated ( $\#P < 0.05$ ). Hematoxylin and eosin staining of paraffin-embedded retinal sections from 1-year-old treated *Tlcd3b*<sup>-/-</sup> mice injected at (C) P21 and (E) P120 demonstrated photoreceptor preservation in the treated RE compared to the untreated LE. The butterfly plot includes ONL thickness measured from 18 equally spaced positions along the vertical



median of the retina collected (D) 6 months after P21 injection and (F) 3 months after P120 injection. Each dot represents an individual data point plotted over mean  $\pm$  SEM. Cone arrestin staining of paraffin-embedded retinal sections from 1-year-old treated *Tlcd3b*<sup>-/-</sup> mice injected at (G) P21 and (H) P120 demonstrated cone photoreceptor preservation in the treated RE compared to the untreated LE. Position 0 corresponds to the optic nerve head. Error bars denote the SEM. Scale bar: 20  $\mu$ m.

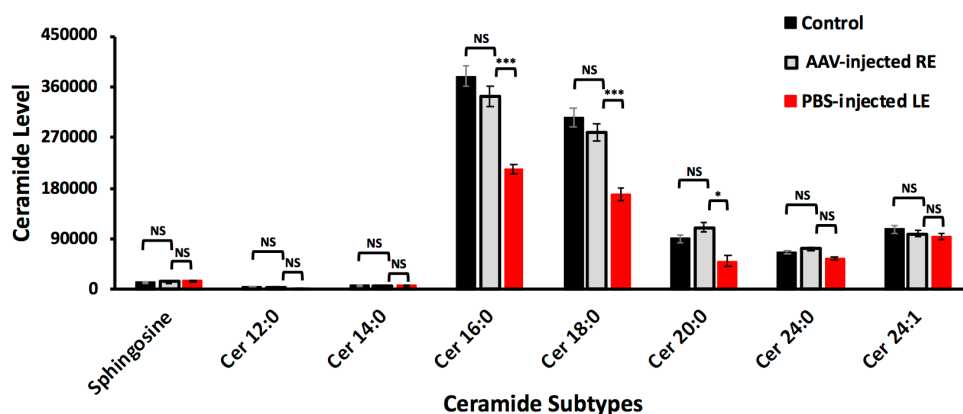


**FIGURE 6.** Mass spectrometric analyses of ceramide species and sphingosine in the retina of *Tlcd3b*<sup>-/-</sup> mice that were treated with *rAAV8-Tlcd3b* gene therapy. All retinas were collected when the P21-injected mice reached 3 months old. Noninjected wild-type mice were used as the external control. The level of sphingolipids was normalized to the total protein content in each sample. All values are mean  $\pm$  SEM, and significance was determined by Student's *t*-test. \**P* < 0.05, \*\**P* < 0.005, \*\*\**P* < 0.001.

*Tlcd3b*<sup>-/-</sup> mice (Fig. 6). Consistent with the idea that TLCD3B functions as a ceramide synthase, in *Tlcd3b*<sup>-/-</sup> mice, the levels of Cer16:0, Cer18:0, and Cer20:0 ceramides were significantly reduced compared to the wild-type control (Fig. 6). *rAAV8-Tlcd3b*-mediated gene therapy at a dosage of  $1.03 \times 10^{12}$  g.c./mL led to a significant increase in the total ceramide level of AAV-injected RE retinas to approximately 90% of that of wild-type control. Specifically, when comparing the treated REs to the PBS-injected LE retina of *Tlcd3b*<sup>-/-</sup> mice, we observed a significant increase in the level of Cer16:0, Cer18:0, and Cer20:0 ceramides to a level comparable to that of the control. Additionally, exogenous TLCD3B expression did not affect the level of sphingosine as well as other ceramide subtypes, indicating that *rAAV8-Tlcd3b* gene therapy specifically targets Cer16–20 and restores their normal level in the retina.

## DISCUSSION

Our results demonstrated that *rAAV8-Tlcd3b*-mediated gene replacement therapy alleviated both impaired retinal function and photoreceptor degeneration. In addition, preservation of ERG responses and increased photoreceptor survival were observed in mice up to 1 year of age after just one round of treatment at P21 or P120, indicating that this treatment is effective over a wide treatment time window, even after a prolonged period of time. This strong effect of *rAAV8-Tlcd3b* gene therapy can likely be attributed to the high transduction rate, robust expression, and proper localization of *rAAV8-Tlcd3b* in the photoreceptors. Taken together, our study provides strong preclinical evidence for the feasibility of using gene replacement therapies to treat TLCD3B patients by targeting photoreceptor cells.

In contrast to endogenous TLCD3B expression, which is throughout the retina, exogenous *rAAV8-Tlcd3b* is only

expressed in photoreceptor cells. Nevertheless, we observed substantial rescue of retinal degeneration for both treatment time points (P21 and P120) at two observation time points (7M and 12M), as demonstrated by the preservation of photoreceptor structure and function in mutant mice after the gene therapy. Therefore, photoreceptor cell-specific expression of *Tlcd3b* was sufficient to rescue the degenerative phenotypes presented by *Tlcd3b*<sup>-/-</sup> mice, indicating that the primary function of *Tlcd3b* is in photoreceptors while rod-bipolar cell dysfunction might be secondary of photoreceptor degeneration.

*Tlcd3b*<sup>-/-</sup> mice were treated at two different time points, P21 and P120. The two time points are both before the degeneration onset at 7 months old. Nevertheless, compared to P120 treatments, P21 treatments have better therapeutic effects, both in terms of photoreceptor survival and retinal function improvement, which are more evident after a prolonged period. This observation could be explained by the fact that mild regional photoreceptor degeneration starts to present around 4 months old (data not shown), despite significant reductions in ONL thickness, and cone cells are not observed in *Tlcd3b*<sup>-/-</sup> mice before 7 months old.<sup>15</sup> As a result, a minority of photoreceptors that are already in their degenerative phase will have a comparatively worse condition to start with and hence end up with a more impaired function and morphology compared to the majority of cells that move slowly into degeneration and/or be less responsive to the gene replacement therapy given their disrupted local environment.<sup>27,37,38</sup> It is also likely that it is harder to infect the photoreceptors of middle-aged mice (P120) than young mice (P21).

In this study, we also validated TLCD3B's role as a ceramide synthase in vivo, as *Tlcd3b*<sup>-/-</sup> mice demonstrated a significant reduction in the levels of C16-, C18-, and C20-ceramides, which agrees with what was shown by the in vitro TLCD3B study.<sup>14</sup> TLCD3B has been demonstrated

to be the most highly expressed ceramide synthase in the retina relative to other six canonical ceramide synthases,<sup>15</sup> and the importance of ceramide homeostasis in retinal neurons has been implicated in several studies.<sup>8–11</sup> Here, we demonstrated that a reduction in ceramide levels also triggers photoreceptor cell death, leading to retinal degeneration. The photoreceptor degeneration phenotype is sensitive to the ceramide levels as stronger rescue is observed when a higher dosage of *rAAV8-Tlcd3b* is used. The downregulation of TLC3B, aside from leading to a reduced level of ceramides in general, also contributes to a shift in the retinal ceramide species ratio, further disrupting sphingolipid homeostasis in the retina. Acting as a metabolic hub within the highly complex network of interconnected sphingolipid metabolism pathways, ceramide occupies a central position in both biosynthesis and catabolism.<sup>7</sup> The disruption of ceramide profiles in the retina may lead to complicated downstream impact in terms of different sphingolipids involved, such as sphingosine-1-phosphate, ceramide-1-phosphate, and sphingomyelin, and the downregulation or upregulation of each sphingolipid species has its specific impact. Future studies will examine the role of TLC3B in ceramide and sphingolipid synthesis pathways and its involvement in the maintenance of photoreceptor function and survival.

In conclusion, our results highlight the success of the first *rAAV8-Tlcd3b*-based gene therapy in *Tlcd3b*<sup>-/-</sup> mouse models of retinopathy. In particular, *Tlcd3b*<sup>-/-</sup> mice showed preservation of the photoresponses as well as a higher survival rate of photoreceptor cells, at both 7 months and 1 year old, demonstrating the prolonged effectiveness of *rAAV8-Tlcd3b* treatment. Findings from this study show that gene replacement therapy in the retina with *rAAV8-Tlcd3b* can improve photoreceptor function in *Tlcd3b*<sup>-/-</sup> mice, extend survival of photoreceptors in vivo, and be potentially used as a therapeutic target for the treatment of patients with retinopathies.

### Acknowledgments

The authors thank the Gene Vector Core at the Baylor College of Medicine.

Supported by the Foundation Fighting Blindness (BR-GE-0613-0618-BCM) and the National Eye Institute (R01EY022356, R01EY020540) to RC.

Disclosure: **X. Qian**, None; **H. Liu**, None; **S. Fu**, None; **J. Lu**, None; **Y.-T. Hung**, None; **C. Turner**, None; **H. Gu**, None; **R. Chen**, None

### References

- Chang GQ, Hao Y, Wong F. Apoptosis: final common pathway of photoreceptor death in rd, rds, and rhodopsin mutant mice. *Neuron*. 1993;11:595–605.
- Portera-Cailliau C, Sung CH, Nathans J, Adler R. Apoptotic photoreceptor cell death in mouse models of retinitis pigmentosa. *Proc Natl Acad Sci USA*. 1994;91:974–978.
- Carella G. Introduction to apoptosis in ophthalmology. *Eur J Ophthalmol*. 2003;13(suppl 3):S5–S10.
- German OL, Miranda GE, Abrahan CE, Rotstein NP. Ceramide is a mediator of apoptosis in retina photoreceptors. *Invest Ophthalmol Vis Sci*. 2006;47:1658–1668.
- Prado Spalm FH, Vera MS, Dibo MJ, Simón MV, Politi LE, Rotstein NP. Ceramide induces the death of retina photoreceptors through activation of parthanatos. *Mol Neurobiol*. 2019;56:4760–4777.
- Sanvicens N, Cotter TG. Ceramide is the key mediator of oxidative stress-induced apoptosis in retinal photoreceptor cells. *J Neurochem*. 2006;98:1432–1444.
- Ranty M-L, Carpentier S, Cournot M, et al. Ceramide production associated with retinal apoptosis after retinal detachment. *Graefes Arch Clin Exp Ophthalmol*. 2009;247:215–224.
- Strettoi E, Gargini C, Novelli E, et al. Inhibition of ceramide biosynthesis preserves photoreceptor structure and function in a mouse model of retinitis pigmentosa. *Proc Natl Acad Sci USA*. 2010;107:18706–18711.
- Zhao L, Spassieva SD, Jucius TJ, et al. A deficiency of ceramide biosynthesis causes cerebellar Purkinje cell neurodegeneration and lipofuscin accumulation. *PLoS Genet*. 2011;7:e1002063.
- Kitatani K, Idkowiak-Baldys J, Hannun YA. The sphingolipid salvage pathway in ceramide metabolism and signaling. *Cell Signal*. 2008;20:1010–1018.
- Hannun YA, Obeid LM. Principles of bioactive lipid signalling: lessons from sphingolipids. *Nat Rev Mol Cell Biol*. 2008;9:139–150.
- Levy M, Futerman AH. Mammalian ceramide synthases. *IUBMB Life*. 2010;62:347–356.
- Wegner M-S, Schiffmann S, Parnham MJ, Geisslinger G, Groesch S. The enigma of ceramide synthase regulation in mammalian cells. *Prog Lipid Res*. 2016;63:93–119.
- Yamashita-Sugahara Y, Tokuzawa Y, Nakachi Y, et al. Fam57b (family with sequence similarity 57, member B), a novel peroxisome proliferator-activated receptor  $\gamma$  target gene that regulates adipogenesis through ceramide synthesis. *J Biol Chem*. 2013;288:4522–4537.
- Bertrand RE, Wang J, Xiong KH, et al. Ceramide synthase TLC3B is a novel gene associated with human recessive retinal dystrophy. *Genet Med*. 2021;23:488–497.
- Schön C, Sothilingam V, Mühlfriedel R, et al. Gene therapy successfully delays degeneration in a mouse model of PDE6A-linked retinitis pigmentosa (RP43). *Hum Gene Ther*. 2017;28:1180–1188.
- Ocelli LM, Schön C, Seeliger MW, Biel M, Michalakakis S, Petersen-Jones SM. Gene supplementation rescues rod function and preserves photoreceptor and retinal morphology in dogs, leading the way toward treating human PDE6A-retinitis pigmentosa. *Hum Gene Ther*. 2017;28:1189–1201.
- Mowat FM, Ocelli LM, Bartoe JT, et al. Gene therapy in a large animal model of PDE6A-retinitis pigmentosa. *Front Neurosci*. 2017;11:342.
- Molday LL, Djajadi H, Yan P, et al. RD3 gene delivery restores guanylate cyclase localization and rescues photoreceptors in the Rd3 mouse model of Leber congenital amaurosis 12. *Hum Mol Genet*. 2013;22:3894–3905.
- Mihelec M, Pearson RA, Robbie SJ, et al. Long-term preservation of cones and improvement in visual function following gene therapy in a mouse model of Leber congenital amaurosis caused by guanylate cyclase-1 deficiency. *Hum Gene Ther*. 2011;22:1179–1190.
- Koch S, Sothilingam V, Garcia Garrido M, et al. Gene therapy restores vision and delays degeneration in the CNGB1(-/-) mouse model of retinitis pigmentosa. *Hum Mol Genet*. 2012;21:4486–4496.
- Boye SL, Conlon T, Erger K, et al. Long-term preservation of cone photoreceptors and restoration of cone function by gene therapy in the guanylate cyclase-1 knockout (GC1KO) mouse. *Invest Ophthalmol Vis Sci*. 2011;52:7098–7108.
- Boye SE, Boye SL, Pang J, et al. Functional and behavioral restoration of vision by gene therapy in the guanylate cyclase-1 (GC1) knockout mouse. *PLoS One*. 2010;5:e11306.
- Jacobson SG, Acland GM, Aguirre GD, et al. Safety of recombinant adeno-associated virus type 2-RPE65 vector delivered

- by ocular subretinal injection. *Mol Ther.* 2006;13:1074–1084.
25. Petersen-Jones SM, Occelli LM, Winkler PA, et al. Patients and animal models of CNG $\beta$ 1-deficient retinitis pigmentosa support gene augmentation approach. *J Clin Invest.* 2018;128:190–206.
  26. Zaneveld SA, Eblimit A, Liang Q, et al. Gene therapy rescues retinal degeneration in receptor expression-enhancing protein 6 mutant mice. *Hum Gene Ther.* 2019;30:302–315.
  27. Zhong H, Eblimit A, Moayed Y, et al. AAV8(Y733F)-mediated gene therapy in a Spata7 knockout mouse model of Leber congenital amaurosis and retinitis pigmentosa. *Gene Ther.* 2015;22:619–627.
  28. Dias MF, Joo K, Kemp JA, et al. Molecular genetics and emerging therapies for retinitis pigmentosa: basic research and clinical perspectives. *Prog Retin Eye Res.* 2018;63:107–131.
  29. Weleber RG, Pennesi ME, Wilson DJ, et al. Results at 2 years after gene therapy for RPE65-deficient Leber congenital amaurosis and severe early-childhood-onset retinal dystrophy. *Ophthalmology.* 2016;123:1606–1620.
  30. Le Meur G, Lebranchu P, Billaud F, et al. Safety and long-term efficacy of AAV4 gene therapy in patients with RPE65 Leber congenital amaurosis. *Mol Ther.* 2018;26:256–268.
  31. Bennett J, Wellman J, Marshall KA, et al. Safety and durability of effect of contralateral-eye administration of AAV2 gene therapy in patients with childhood-onset blindness caused by RPE65 mutations: a follow-on phase 1 trial. *Lancet.* 2016;388:661–672.
  32. Georgiadis A, Duran Y, Ribeiro J, et al. Development of an optimized AAV2/5 gene therapy vector for Leber congenital amaurosis owing to defects in RPE65. *Gene Ther.* 2016;23:857–862.
  33. Petrs-Silva H, Dinculescu A, Li Q, et al. High-efficiency transduction of the mouse retina by tyrosine-mutant AAV serotype vectors. *Mol Ther.* 2009;17:463–471.
  34. Ku CA, Chiodo VA, Boye SL, et al. Gene therapy using self-complementary Y733F capsid mutant AAV2/8 restores vision in a model of early onset Leber congenital amaurosis. *Hum Mol Genet.* 2011;20:4569–4581.
  35. Pang JJ, Dai X, Boye SE, et al. Long-term retinal function and structure rescue using capsid mutant AAV8 vector in the rd10 mouse, a model of recessive retinitis pigmentosa. *Mol Ther.* 2011;19:234–242.
  36. Zhong H, Eblimit A, Moayed Y, et al. AAV8(Y733F)-mediated gene therapy in a Spata7 knockout mouse model of Leber congenital amaurosis and retinitis pigmentosa. *Gene Ther.* 2015;22:619–627.
  37. Cideciyan AV, Jacobson SG, Beltran WA, et al. Human retinal gene therapy for Leber congenital amaurosis shows advancing retinal degeneration despite enduring visual improvement. *Proc Natl Acad Sci USA.* 2013;110:E517–E525.
  38. Botto C, Rucli M, Tekinsoy MD, Pulman J, Sahel J-A, Dalkara D. Early and late stage gene therapy interventions for inherited retinal degenerations. *Prog Retin Eye Res.* 2021;86:100975.